SYNTHESIS AND MAGNETIC PROPERTIES OF CHROMIUM-BASED $Cu(Cr_{2-x}Ti_x)S_4$ THIOSPINELS AND THEIR DEFICIENT STRUCTURES $Cu_{1-y}\square_yCr_{2-x}Ti_xS_4$ OBTAINED BY COPPER EXTRACTION

PATRICIA BARAHONA [a], ANTONIO GALDAMEZ [b], FERNANDA LOPEZ-VERGARA [b], VÍCTOR MANRIQUEZ [b], OCTAVIO PEÑA [c]*

[a] *Facultad de Ciencias Básicas, Universidad Católica del Maule, Talca, Chile*
[b] *Departamento de Química, Facultad de Ciencias, Universidad de Chile, Santiago, Chile*
[c] *Institut des Sciences Chimiques de Rennes, UMR 6226, Université de Rennes 1, Rennes, France*
(Received: March 5, 2013 - Accepted: September 6, 2013)

ABSTRACT

The crystalline structure of spinels is extremely flexible due to the presence of several sublattices in which the cations can be distributed and localized in different crystallographic sites depending on their sizes, oxidation states or coordination numbers. Cationic substitution and ions-extraction are appropriate tools to change the oxidation state inside the spinel structure, thus substantially modifying the magnetic properties. The spinel sulfide $CuCr_2S_4$ is a metallic ferromagnet with T_C = 377 K, where Cr is mixed-valence Cr^{3+}/Cr^{4+}, while $CuTi_2S_4$ is a Pauli paramagnet, with Ti in a mixed-valence state (singlet ground state for Ti^{3+} ; non-magnetic, S = 0, state for Ti^{4+}). The copper ion Cu^+ is in a closed-shell configuration. The mixed spinel $CuCr_{2-x}Ti_xS_4$ gives the possibility to change the oxidation state of Cr ions when titanium ions are introduced. Another way to control the oxidation state of the ions is by copper extraction from the lattice, thus producing a change in the magnetic behavior of the material.

We report the synthesis, crystallographic and magnetic properties of the solid solution $CuCr_{2-x}Ti_xS_4$ and its deficient-spinel structure obtained by copper extraction. Powder samples of $CuCr_{2-x}Ti_xS_4$ were prepared in quartz ampoules at 900 °C. Deficient spinels $Cu_{1-y}\square_yCr_{2-x}Ti_xS_4$ were prepared by mild treatment with oxidizing agents such as iodine in acetonitrile at 50 °C.

Keywords: Ferrimagnetic Perovskites, Thiospinel, Copper extraction, Mixed valence Cr.

1. INTRODUCTION

The discovery of the colossal magneto-resistance CMR effect has attracted a renew interest in manganites perovskites $LnMnO_3$ (Ln = lanthanide) partially substituted at the A-site by an alkaline earth metal, $Ln_{1-x}A_xMnO_3$, due to their potential technological applications in the manufacture of electronic devices [1-3]. The essential physical mechanisms of the CMR phenomena in these manganites are believed to be the double-exchange (DE) and Jahn-Teller (JT) effects, both intimately related to the mixed-valence character of the Mn cation [4]. However, in chromium-based chalcogenide materials of spinel structure ACr_2S_4 (A = transition metal), also identified as CMR materials, there are neither heterovalence nor JT effect [5]. Thus, it becomes very interesting to look deeper onto the magnetic ordering and the interaction mechanisms which might exist between the two (or more) magnetic sublattices coexisting in the spinel structure.

The magnetic and transport properties in chalcogenide spinels ACr_2S_4 are strongly influenced by the distribution of the metal ions in the structure. This is essentially related to (i) the existence of two types of cationic sites, tetrahedral (*A*) and octahedral (*B*); and (ii) the great flexibility of the structure in hosting various metal ions, differently distributed between sites, with a large possibility of substitution between them. As the cationic distribution can change when substitution occurs, the physical properties of the spinel material may strongly differ from those of the non-substituted compound. Therefore, solid solutions of thiospinels have received considerable attention for their interesting electrical and magnetic properties, which can greatly vary as a function of composition [6-8].

The chalcogenide spinel $CuCr_2S_4$ crystallizes in a normal spinel structure (space group *Fd*-3*m*), in which Cu and Cr ions occupy the tetrahedral *A* and octahedral *B* sites, respectively. $CuCr_2S_4$ is a metallic ferromagnet, with ordering temperature T_c of about 377 K [9-11]. Lotgering et al. have explained the properties of $CuCr_2S_4$ assuming that the charge distribution in this compound should be represented as $Cu^+Cr^{3+}Cr^{4+}S_4$ in which the metallic conduction and ferromagnetism have been attributed to double exchange between Cr^{3+} and Cr^{4+} [12]. On the other hand, Goodenough suggested a model with Cu^{2+} and Cr^{3+} ions with some ferromagnetic interactions between Cr ions [13]. In contrast, Yamashita et al [14] and Schöllhorn [15] explained its metallic behavior in terms of anionic mixed valence $(Cu^+Cr_2^{3+}(S^{2-})_3S^-)$, with delocalized holes in the sulfur valence band giving rise to the observed metallic behavior. By using magnetic circular dichroism and X-ray photoemission spectroscopy, Kimura et al showed the presence of monovalent copper at room temperature superposed to a weak spin paramagnetic moment at the copper site, implying the presence of a small amount of Cu^{2+} [16]. To reconcile all these various models, Kamihara et al suggested an electronic structure as $Cu^+_{1-n}Cu^{2+}_nCr^{3+}_{1+n}Cr^{4+}_{1-n}S^{2-}_4$ in which *n* gradually decreases to 0 with increasing temperature [17]. More recently, Bodenez et al, using high resolution electron energy loss spectroscopy, suggested $Cu^+Cr_2^{3+}(S^{-2})_3S^-$ as the oxidation state of the pristine material [18].

The cubic thiospinel $CuTi_2S_4$ can be formally described as $Cu^+Ti^{3+}Ti^{4+}S_4$ with non-magnetic Cu^+ and mixed-valence Ti (Ti^{3+} and Ti^{4+}). This compound is known to display a Pauli paramagnetism and a spin singlet ground state [19,20] and behaves as a metal in terms of its electronic structure and transport properties [13].

The small size of the monovalent Cu^+ ion allows its easy extraction from $CuTi_2S_4$ and $CuCr_2S_4$. In the case of $CuTi_2S_4$ this can be done by using oxidizing agents like I_2 or Br_2 in acetonitrile, producing the cation deficient compound $\square_yTi_2S_4$. However, this method is not possible in $CuCr_2S_4$. The copper extraction in $CuCr_2S_4$ can be done by using n-butyl lithium in hexane, thus producing $Li_zCu_{1-y}\square_yCr_2S_4$. These methods were successfully used to elaborate these materials as cathodes for lithium secondary batteries [21-23]. In our case, we are mostly interested in the possibility to modify the oxidation state of the cations by extracting copper from the synthesized $CuCr_{2-x}Ti_xS_4$ phases and thus inducing modifications to the magnetic behavior of these thiospinels.

In this paper, we report on mixed-cation phases $CuCr_{2-x}Ti_xS_4$ ($0.3 < x \leq 2.0$), prepared at 900 °C in evacuated quartz tubes, subsequently dissolved in a iodine-based solution to form a material of general formula $Cu_{1-y}\square_yCr_{2-x}Ti_xS_4$. The aim of this work is to study the influence on the magnetic properties of both the partial substitution at the B-site of the $CuCr_2S_4$ ferromagnetic thiospinel and the soft-chemical extraction of Cu at the A-site. In this way, it becomes easy to modulate the oxidation state of cations in the chalcogenide spinel, either by partial substitution of Cr by Ti in the solid solution $CuCr_{2-x}Ti_xS_4$ or by introducing vacancies at the copper site, in the deficient $Cu_{1-y}\square_yCr_{2-x}Ti_xS_4$ spinel structure. Materials are characterized by crystallochemical and magnetization techniques, both before and after creation of vacancies.

2. EXPERIMENTAL

Polycrystalline samples of $CuCr_{2-x}Ti_xS_4$ ($0.3 < x \leq 2.0$) were prepared by solid-state reaction method. High purity powders of copper (Aldrich, 99%), chromium (Sigma-Aldrich, 99.5%), titanium (Aldrich, 99.9) and sulfur (Sigma-Aldrich, 99.98%) were mixed according to the stoichiometric ratio with 3wt% excess S. The mixed powder samples were pressed into pellets, sealed into evacuated quartz tubes, and heated to 900 °C (1173 K) at the rate of 0.3 °C/min for 2 weeks. All samples were furnace-cooled after the firing. X-ray powder diffraction (XRD) data collection was performed in the range $5° < 2\theta < 90°$ on a Siemens D 5000 powder diffractometer with Cu-K_α radiation.

e-mail: pbaraho@ucm.cl

Elemental analyses, performed by SEM-EDX on a JEOL 6400 SEM equipped with Oxford Link Isis EDX detector, showed a good agreement (within 5 %) with the expected compositions. Magnetic measurements were performed on pelletized powder samples using a Quantum Design MPMS XL5 SQUID magnetometer as a function of temperature in the range [2-300 K] (zero field cooled/field cooled ZFC/FC cycles at low fields, and magnetic susceptibility in the paramagnetic state, under high fields) and as a function of applied field M(H) at T = 2 K.

Copper extraction was performed using similar techniques as those previously reported for $CuTi_2S_4$ [21], i.e. by oxidation of the starting material with I_2 in acetonitrile as the oxidation reagent, to obtain a product of nominal composition $Cu_{1-y}\square_yCr_{2-x}Ti_xS_4$. More specifically, to carry out the reaction, we suspended about 300 mg of $CuCr_{2-x}Ti_xS_4$ in an excess of 0.1 M I_2/CH_3CN (75 mL) product solution at 50 °C while magnetic stirring for a period of four days. The solid product was then washed with dry acetonitrile and stored.

3. Structure and microstructure

3.1. X-ray diffraction

The XRD patterns were fully indexed in the space group *Fd-3m*, with no secondary phases observed within the limits (less than 5 %) of the experimental detection of both SEM-EDX and XRD analyses. Representative diffraction profiles are shown in Fig. 1. The substitution of chromium by titanium in $CuCr_{2-x}Ti_xS_4$ results in crystalline phases with structures identical to the one of $CuTi_2S_4$ [19]. The values of the cell parameter, *a*, for all compounds are given in Table 1. The *a* parameter, related to the non-substituted compound increases when titanium replaces part of chromium (a = 9.814 Å for $CuCr_2S_4$ [9], a = 10.000 Å for $CuTi_2S_4$ [19]).

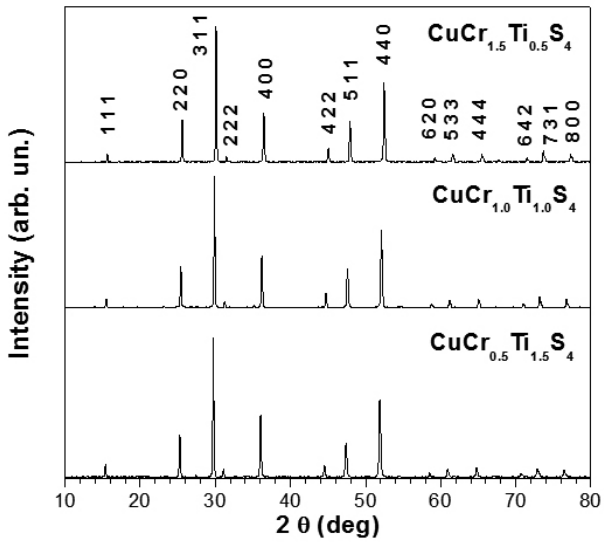

Figure 1. XRD patterns of $CuCr_{1.5}Ti_{0.5}S_4$, $CuCr_{1.0}Ti_{1.0}S_4$ and $CuCr_{0.5}Ti_{1.5}S_4$.

Table 1. Crystallographic and magnetic data for the solid solution $Cu(Cr_{2-x}Ti_x)S_4$. Space group *Fd-3m*.

x(Ti)	Compound	*a* (Å)	μ_{eff} ± 0.05 (μ_B)	θ ± 5 K (K)	T_C ± 2 K (K)	M (50 kOe,2 K) # (μ_B)
Ferromagnetic regime						
0.0	$CuCr_2S_4$ [11,12]	9.814 [9]	4.58		377	4.04
0.3	$Cu(Cr_{1.7}Ti_{0.3})S_4$	9.8200	4,03	+ 312	291 (a)	3.84
0.5	$Cu(Cr_{1.5}Ti_{0.5})S_4$	9.8674	4,09	+ 247	226 (a)	3.65
0.7	$Cu(Cr_{1.3}Ti_{0.7})S_4$	9.8732	3,97	+ 173	149 (a)	3.03
Reentrant and spin-glass regime						
1.0	$Cu(Cr_{1.0}Ti_{1.0})S_4$	9.9362	3,64	+ 63	52.5 (b)	0.95
1.3	$Cu(Cr_{0.7}Ti_{1.3})S_4$	9.9557	3,11	+ 39	11.5 (b)	0.93
1.5	$Cu(Cr_{0.5}Ti_{1.5})S_4$	9.9747	2,66	+ 51	7.7 (b)	0.89
Paramagnetic regime						
1.7	$Cu(Cr_{0.3}Ti_{1.7})S_4$	9.9791	TIP *	- - -	- - -	0.54
2.0	$CuTi_2S_4$	10.000 [19]	TIP *	- - -	- - -	0.01

value of the magnetization taken at T = 2 K and H_{app} = 50 kOe
* TIP = Temperature Independent Paramagnetism
(a) T_C values from extrapolation to M = 0 of the M^{FC} curve
(b) T_C values from derivative of the M^{FC} curve

3.2. Chemical Extraction of Copper

The extraction of copper using I_2-CH_3CN was performed in the series $CuCr_{2-x}Ti_xS_4$ ($0.3 < x \leq 2.0$). The results suggest that, if the initial thiospinels are rich in titanium (x > 1.0, i.e. above 50 % occupation of the B-site), then the copper can be extracted to give a cationic deficient compound (Table 2). This is possible since the presence of titanium at a 3+ valence state allows its oxidation as Ti^{4+}, with simultaneous copper extraction when x > 1.0 [24,25]. Therefore the presence of large amounts of titanium in the compound is essential to achieve the extraction of copper.

Table 2. Copper extraction of solid solution $Cu(Cr_{2-x}Ti_x)S_4$ using I_2-CH_3CN as oxidation reagent. EDX analysis within 5 %.

x(Ti)	Nominal composition	EDX analysis of starting compounds	EDX analysis of copper-deficient compounds (a)
0.3	$Cu(Cr_{1.7}Ti_{0.3})S_4$	$Cu_{1.06}(Cr_{1.61}Ti_{0.32})S_{3.82}$	No reaction
0.5	$Cu(Cr_{1.5}Ti_{0.5})S_4$	$Cu_{1.01}(Cr_{1.55}Ti_{0.50})S_{3.89}$	No reaction
0.7	$Cu(Cr_{1.3}Ti_{0.7})S_4$	$Cu_{1.02}(Cr_{1.29}Ti_{0.70})S_{3.82}$	No reaction
1.0	$Cu(Cr_{1.0}Ti_{1.0})S_4$	$Cu_{1.00}(Cr_{0.99}Ti_{1.01})S_{4.03}$	No reaction
1.3	$Cu(Cr_{0.7}Ti_{1.3})S_4$	$Cu_{1.04}(Cr_{0.68}Ti_{1.31})S_{4.04}$	$Cu_{0.60}\square_{0.40}(Cr_{0.64}Ti_{1.30})S_4$
1.5	$Cu(Cr_{0.5}Ti_{1.5})S_4$	$Cu_{1.01}(Cr_{0.49}Ti_{1.49})S_{4.09}$	$Cu_{0.49}\square_{0.51}(Cr_{0.48}Ti_{1.50})S_4$

(a) Compositions normalized to the nominal Ti content

The XRD data of the copper-extracted product $Cu_{1-y}\square_yCr_{2-x}Ti_xS_4$ are similar to the starting compounds $CuCr_{2-x}Ti_xS_4$, without presence of secondary phases (Fig. 2). Final compositions of the copper-extracted samples were obtained by SEM-EDX analysis and are given in Table 2.

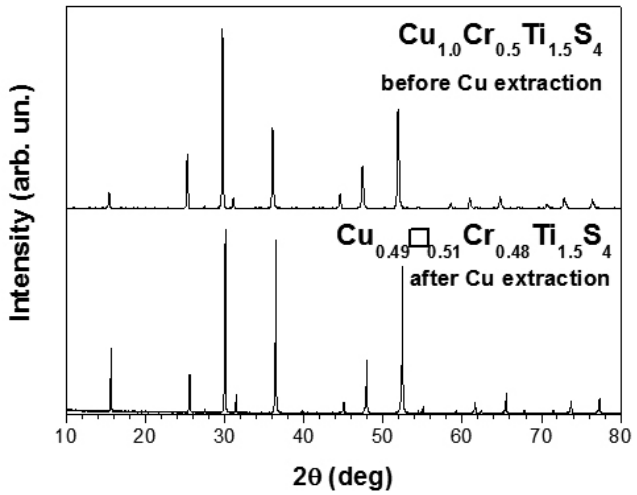

Figure 2. XRD patterns of copper deficient Cu0.49□0.51Cr0.48Ti1.50S4 (bottom) obtained by coppter extraction from $Ru_{1-0}Cr_{0.5}Ti_{1.5}S_4$ (top). Compositions as obtained by SEM-EDX analysis.

4. Magnetic behavior

The solid solution under investigation is extremely rich in magnetic phenomena, and constitutes a model system in many aspects. Firstly, the limiting compounds $CuCr_2S_4$ and $CuTi_2S_4$ represent a ferromagnetic and a Pauli paramagnetic limits, respectively, in which both Ti and Cr can be considered in mixed-valence states. However, Ti^{3+} (S = ½) is in a singlet state with no intrinsic effective moment, while Cu has a closed shell (Cu^+; S = 0) [20,26]. Then, all magnetic behavior is due to the chromium contribution, which may be under different configurations, depending on the degree of substitution [27]. Secondly, the progressive substitution of chromium by titanium allows to cover different domains of the magnetic phase diagram, in particular, the spin-glass regime and its different variants (diluted regime, pure spin-glass, coexistence of ferromagnetism and spin-glass). In particular, the spin-glass phenomenon appears to exist in a very narrow range of substitutions around x = 1.0 [27]. Finally, the coexistence phenomenon, in which both ferromagnetism and antiferromagnetism are simultaneously present in the sample, constitutes a good test for theoretical studies, such as the Gabay-Thoulouse [28] and the Almeida-Thouless [29] models.

Our goal is to investigate some specific samples which characterize the different species within the magnetic-phase diagram of the solid solution. For these samples, extraction of copper from the crystallographic lattice allows to greatly modify the electronic structure of the starting material, triggering additional interaction mechanisms due to a modification of the oxidation states of the constituent elements.

4.1. $Cu(Cr_{2-x}Ti_x)S_4$ solid solution

4.1.i) ferromagnetic regime

Three characteristic compositions of the ferromagnetic regime in the $Cu(Cr_{2-x}Ti_x)S_4$ solid solution were synthesized, x = 0.3, x = 0.5 and x = 0.7. Figure 3 shows our results, recorded in the ZFC/FC modes, under an applied field of 500 Oe. The ferromagnetic Curie temperature T_C (extrapolated value to M = 0, of the linear increase of $M^{FC}(T)$ when cooling), decreases abruptly with increasing x, going from 291 to 149 K (Table 1). The ZFC and FC branches almost perfectly overlap, although a very slight irreversibility (less than 1 %) can be observed at the lowest temperatures (insert, Figure 3), which we consider as negligible. We also notice for sample x = 0.3, an anomaly at 45 K, very similar although less intense, to data reported by Kariya et al and tentatively attributed to domain-wall blocking [27].

Measurements performed at T = 2 K as a function of field give saturation moments M_{sat} of 3.84, 3.65 and 3.03 μ_B for x = 0.3, 0.5 and 0.7, respectively (Figure 4 and Table 1). The fast drop of M_{sat}, when going from x = 0.5 to 0.7, announces a change in the magnetic regime, to be discussed later. As it can be readily noticed from figure 4, sample $CuCr_{1.3}Ti_{0.7}S_4$ is at the compositional limit of ferromagnetism. Attempts to determine the Curie constant C and the associated effective moment (μ_{eff} = v8xC) were done in a narrow temperature range ($T_C < T < 400$ K) ; results are reported in Table 1. It is to be noticed that application of a high field (H_{app} = 10 kOe) was necessary in order to get large enough signals, with no background noise. However, the limited range of temperatures available for a Curie-Weiss fit of the experimental data gives large uncertainties to the magnetic parameters reported in Table 1.

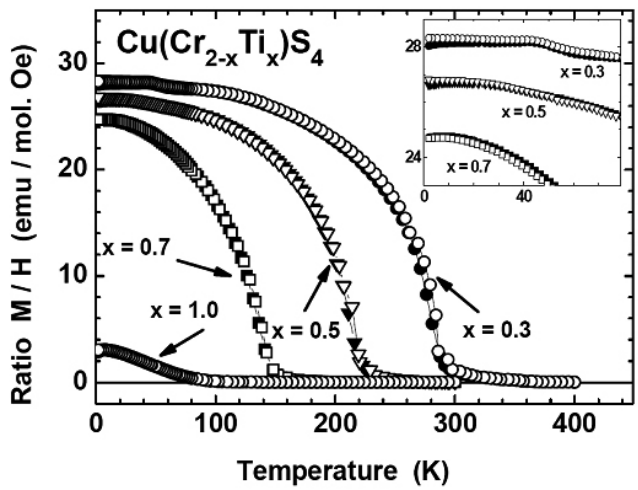

Figure 3. ZFC/FC magnetization cycles measured at Happ = 500 Oe for given solid solutions $CuCr_2$ $xTixS_4$ in the ferromagnetic regime (ZFC : filled symbols / FC : open symbols). Insert zooms low temperature data. Sample x = 1.0 is included for comparison (more details in Figure 5).

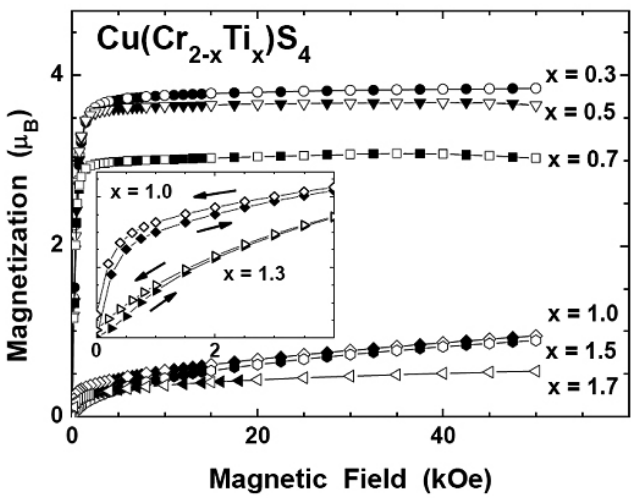

Figure 4. Magnetization measured at 2 K for given solid solutions $CuCr_{2-x}Ti_xS_4$ under increasing (filled symbols) and decreasing (open symbols) applied fields.

4.1.ii) reentrant and spin-glass regime

Two samples belonging to the spin-glass regime were studied in this work. The first one, x = 1.0 ($CuCrTiS_4$), is at the limiting range of the coexistence phenomenon between ferromagnetism and spin-glass. The second one, x = 1.3 ($CuCr_{0.7}Ti_{1.3}S_4$), should be, according to ref. 26, a typical example of a spin-glass system.

Before going into details of the temperature dependence of the magnetization (ZFC/FC cycles), we call the attention into the magnetization as a function of field (M-H curves), as represented in figure 4. From this figure, the spectacular decrease of the magnetization, when going from x = 0.7 to x

= 1.0, points out to the existence of new mechanisms of magnetic interaction developing in the sample. A look at the field dependence at high fields (sample with x = 1.3 is not shown in the main panel for sake of clarity), allows to identify two main mechanisms of interaction: one due to a ferromagnetic contribution which tends to saturate rather fast with the applied field, and an antiferromagnetic contribution, with M increasing rather linearly with H_{app} (insert, Fig. 4). From these observations we may conclude that both samples $CuCr_{1.0}Ti_{1.0}S_4$ and $CuCr_{0.7}Ti_{1.3}S_4$, belong to a regime of mixed ferro- and antiferro-magnetic behaviors, probably due to the formation of ferromagnetic clusters which interact antiferromagnetically with each other. Insert, figure 4 shows indeed a weak magnetic hysteresis and negligible coercive fields, typical of ferromagnetic domains.

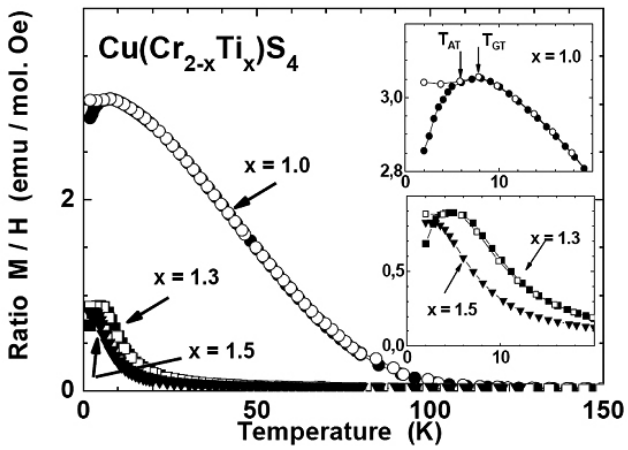

Figure 5. ZFC/FC magnetization cycles measured at H_{app} = 500 Oe. Inserts show details for samples presenting: coexistence of ferromagnetism and spin-glass (x = 1.0), spin-glass (x = 1.3) and superposition of spin-glass and paramagnetic (x = 1.5) behaviours.

Figure 5 shows the ZFC/FC cycles, in the temperature ranges $2 \leq T \leq 150$ K (main panel) and $2 \leq T \leq 20$ K (inserts), for the two samples belonging to the reentrant and spin-glass regimes (x = 1.0 and 1.3). At a first look, sample $CuCr_{1.0}Ti_{1.0}S_4$ shows some intermediate behavior between a ferromagnetic limit (x < 1.0) and antiferromagnetic or diluted spin-glass thermal variation (x > 1.0), that is, the overall magnetization seems to be a superposition of both regimes. Indeed, it is absolutely remarkable the fact that the magnetization at T = 0 (that is, the extrapolation of M^{FC} to the Y-axis) for this composition drops suddenly by a factor of 10, between samples belonging to the ferromagnetic regime (x < 1.0) and this one, corresponding to the mixed reentrant state (x = 1.0), as shown in figure 3. By the same consideration, this extrapolated value at T = 0 drops further (factor ÷3) between sample x = 1.0 and those characterizing the spin-glass regime and paramagnetic behaviors (x > 1.0), as shown in figure 5. This means that qualitative changes take place, for which sample $CuCrTiS_4$ is a special case limiting two (or more) different magnetic regimes.

To further confirm this qualitative change, the upper insert, figure 5, shows the low temperature ZFC/FC cycle for sample $CuCrTiS_4$ measured under an applied field of 500 Oe. Using the arguments of reference 27, two characteristic temperatures are observed: the T_{GT} (or Gabay-Toulouse mixed phases) temperature at 8 K and the T_{AT} (or de Almeida-Thouless irreversible behavior) temperature at ~6K. The first one (T_{GT}) describes the coexistence of a ferromagnetic state and a transverse spin freezing of the spin-glass regime; the second temperature (T_{AT}) describes the spin-glass phase in which the three (x-, y-, and z-) components freeze simultaneously, leading to a strong irreversibility of the ZFC and FC branches of the magnetization. These two temperatures are hardly seen for sample $CuCr_{0.7}Ti_{1.3}S_4$ (lower insert, figure 5), and we may consider that this sample behaves as a classical spin-glass system, with gel temperature T_g of 5 K. The experimental value of T_g (5 K) is almost the same as the one determined for T_{AT} in the previous sample, confirming that we are dealing with the same antiferromagnetic interaction mechanism between clusters, with no spurious ferromagnetic intracluster interaction.

Sample of composition $CuCr_{0.5}Ti_{1.5}S_4$ (x = 1.5) is at the limit of the spin-glass regime. The lower insert, figure 5, shows indeed full reversibility of the ZFC/FC cycle within our experimental temperature range, with a peak-like variation at 2 K which may suggest the existence of a frozen (gel) regime typical of short-range antiferromagnetic interactions. It is quite possible that T_g is lower than 2 K, setting a lower limit to the spin-glass regime. In addition, there is no magnetic hysteresis in the M(H) curve recorded at 2 K (fig. 4) confirming that ferromagnetic Cr-Cr interactions are absent, leaving just the antiferromagnetic interactions within clusters (spin-glass systems) superposed to a paramagnetic regime.

4.1.iii) paramagnetic regime

As discussed before, the upper limit of the solid solution is represented by the titanium-rich samples of the $Cu(Cr_{2-x}Ti_x)S_4$ family, i.e. $CuCr_{0.3}Ti_{1.7}S_4$ (x = 1.7) including the fully-substituted compound $CuTi_2S_4$. This agrees with the magnetic phase diagram reported by Kariya et al, who settled the paramagnetic regime at x > 1.7 [27]. Figure 6 shows the temperature dependence of the last two samples studied in this work: x = 1.7 (insert) and x = 2.0 (main panel). For these samples, the magnetic susceptibility is superposed to a temperature-independent paramagnetism (TIP) which, in the case of x = 2.0, is equal to 2.45×10^{-4} emu/mol, in agreement with values reported in the literature [19]. We should however recall some of the main features regarding $CuTi_2S_4$, in particular a temperature-dependent term coming from the high density of states of the Ti 3d bands at the Fermi level [20,26]. This is fairly well observed in $CuCr_{0.3}Ti_{1.7}S_4$ (x = 1.7), whose magnetic susceptibility (insert, figure 6) resembles to the intrinsic magnetic susceptibility evaluated by Okada et al [20] for the spinel $CuTi_2S_4$ after subtraction of some impurities contribution. We should remark that the thermal dependence of the magnetization of $CuCr_{0.3}Ti_{1.7}S_4$ shows a tendency to reach a plateau at 50 K, as also reported in ref. 20 for the intrinsic magnetic susceptibility of $CuTi_2S_4$. In our case however, the absolute values of the magnetization for the substituted compound (x = 1.7) are much larger than those reported for $CuTi_2S_4$ and therefore, we may conclude that the Ti 3d bands are even narrower than those suggested for the limiting spinel.

Due to these TIP contributions of Pauli [20] or Van-Vleck [26] character, it becomes difficult to evaluate the effective moment of the well-diluted Cr sublattice (0.3 atoms of chromium per formula unit). Considering their M(H) and ZFC/FC behaviors, we can postulate however, that these two samples belong to the paramagnetic regime, with no magnetic interactions.

4.2. Copper extraction and deficient thiospinels

As said before (§.3.2.), copper extraction performed using an iodine solution I_2-CH_3CN was successful only for samples rich in titanium. Other techniques should be tried in the future for the other end of the series to create vacancies at the copper site. Only two deficient-cation samples were thus obtained from initial materials $CuCr_{0.7}Ti_{1.3}S_4$ and $CuCr_{0.5}Ti_{1.5}S_4$, giving place to $Cu_{0.60}\square_{0.40}(Cr_{0.64}Ti_{1.30})S_4$ and $Cu_{0.49}\square_{0.51}(Cr_{0.48}Ti_{1.50})S_4$, respectively, as analyzed by SEM-EDX techniques (Table 2).

Figure 7 shows the low temperature ZFC/FC cycle for sample x = 1.5 before and after copper extraction. It is immediately seen that the overall magnetic moment is reduced by a factor of 4-5, as also observed in the magnetization M(H) data obtained at 2 K (not shown). However, the paramagnetic moment evaluated from a Curie-Weiss fit of the high temperature data does not change (within the experimental uncertainties ± 0.03 μ_B) with respect to the starting material, 2.67 μ_B compared to 2.66 μ_B (Table 3). The most significant change concerns the Curie-Weiss temperature Θ_{CW} which decreases from a positive ferromagnetic-like value (+51 K; Table 1) down to an almost null value (~0 K; Table 3). This means that ferromagnetic interactions within the

Table 3. Magnetic data for deficient spinel $Cu_{1-y}\square_yCr_{2-x}Ti_xS_4$ structures.

x(Ti)	y(□)	Copper-deficient compounds	μ_{eff} ± 0.03 (μ_B)	θ (K)
1.3	0.40	$Cu_{0.60}\square_{0.40}(Cr_{0.64}Ti_{1.30})S_4$	3.13	-1.5
1.5	0.51	$Cu_{0.49}\square_{0.51}(Cr_{0.48}Ti_{1.50})S_4$	2.67	~0

chromium sublattice tend to disappear because of magnetic dilution at the B-site and/or void sites at the A tetrahedral sites. From these two possibilities, the latter seems the most plausible one to explain the weaker exchange interactions between ions located at the B-site. The low-temperature spin-glass regime is not greatly modified, if one compares the insert of figure 7 with the lower insert, figure 5. In both cases, a maximum is observed around 2 K, our lowest limiting temperature, meaning that T_g should be around 2 K or below.

Similar interpretations can be forwarded in the case of the x = 1.3 sample. The magnetic moment slightly increases, from 3.11 to 3.13 μ_B (again, compatible values within the experimental errors) after copper extraction. A significant variation occurs again for Θ_{CW}, which goes from +39 K (Table 1) down to a negative antiferromagnetic-like value of -1.5 K (Table 3). The ZFC/FC magnetizations are reduced by one order of magnitude but the spin-glass

behavior is maintained, with a T_g of 5 K for the starting sample $CuCr_{0.7}Ti_{1.3}S_4$ (fig. 5) and for its counter-partner after copper extraction $Cu_{0.60}\square_{0.40}(Cr_{0.64}Ti_{1.30})S_4$ (figure 8). For this sample, we have performed a.c. measurements as a function of temperature and frequency in order to confirm its spin-glass nature: as expected for spin-glass systems, a clear dependence of the peak position onto the excitation frequency was obtained, as shown in figure 8.

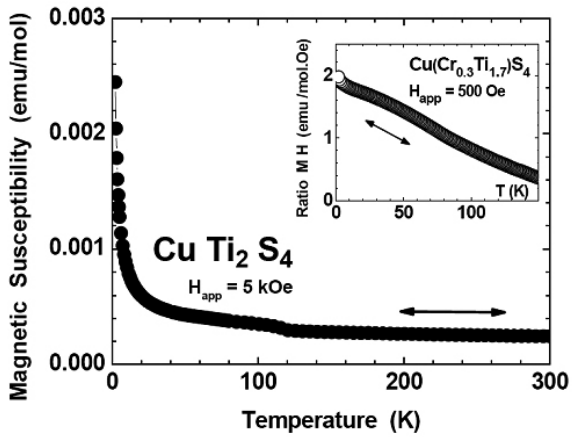

Figure 6. Thermal dependence of the magnetization of given solid solutions $CuCr_{2-x}Ti_xS_4$, measured under an applied field of 500 Oe (x = 1.7) and 5 k Oe (x = 2.0).

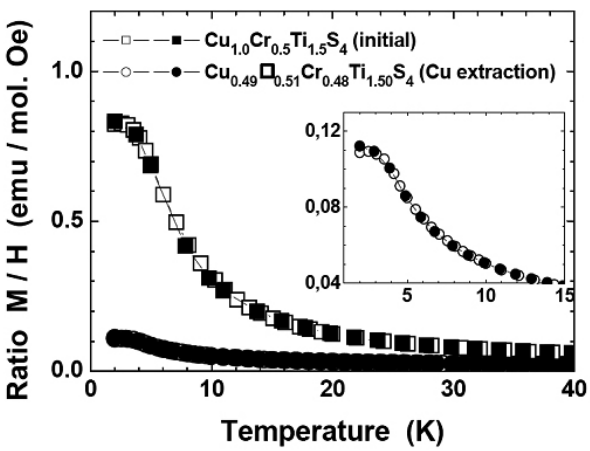

Figure 7. ZFC/FC magnetization cycles measured at Happ = 500 Oe for CuCr0.5Ti1.5S4 and corresponding copper-deficient sample. Insert: low temperature data for Cu0.49□0.51(Cr0.48Ti1.50)S4 (ZFC : open symbols / FC : filled symbols).

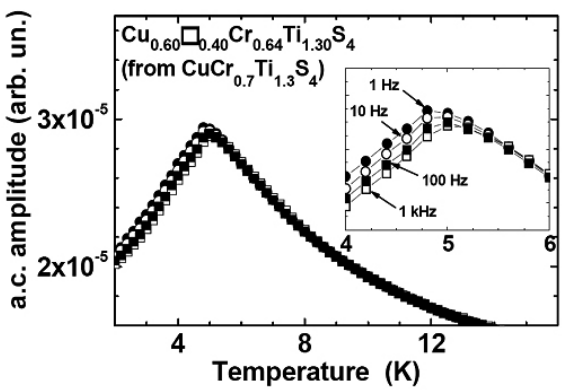

Figure 8. Temperature dependence of the a.c. amplitude of magnetization for a copper-deficient sample $Cu_{0.60}\square_{0.40}(Cr_{0.64}Ti_{1.30})S_4$ derived from $CuCr_{0.7}Ti_{1.3}S_4$

5. CONCLUSIONS

We have investigated the effects of the partial substitution of chromium by titanium on the structural and magnetic properties of $CuCr_2S_4$. We found that the synthesized compounds $CuCr_{2-x}Ti_xS_4$ ($0.3 < x \leq 2.0$) are perfectly homogeneous and they are all indexed in the space group *Fd-3m*. The variation of the lattice parameter is in perfect agreement with the *a* parameter of the non-substituted compound, increasing when titanium replaces part of chromium in $CuCr_{2-x}Ti_xS_4$.

The ZFC/FC and M(H) magnetization cycles on $CuCr_{2-x}Ti_xS_4$ ($0.3 < x \leq 2.0$) show different domains of the magnetic phase diagram, from ferromagnetism (x = 0.3, 0.5, 0.7), coexistence of ferromagnetism and spin-glass (x = 1.0), spin-glass and antiferromagnetic interactions (x = 1.3, 1.5) and finally, paramagnetic behavior (x = 1.7 and 2.0). Ferromagnetic interactions are rapidly lost due to the magnetic dilution of the Cr sublattice, while the presence of vacancies at the Cu-site (ca. 50 % void sites) boosters the antiferromagnetic and spin-glass regimes, with a sharp decrease of the Curie-Weiss Θ_{CW} temperature.

ACKNOWLEDGMENTS

Research financed by grant FONDECYT N° 1110161 and ECOS-CONICYT C09E01. Authors are members of the France-Chile Joint International Laboratory LIA-MIF CNRS N°836.

REFERENCES

1. R. Von Helmolt, J. Wecker, B. Holzapfel, L. Schultz, K. Samwer, *Phys. Rev. Lett*. **71**, 2331, (1993)
2. C.N.R. Rao, B.Raveau (Eds.), *Colossal Magnetoresistance Charge Ordering and Related Properties of Manganese Oxides*, World Scientific, Singapore, 1998.
3. Y. Tokura, *Colossal Magnetoresistive Oxides*, Gordon & Breach, New York, 2000.
4. A. J. Millis, P.B. Littlewood, B.I. Shraiman, *Phys. Rev. Lett.* **74**, 5144, (1995)
5. A.P. Ramirez, R.J. Cava, J. Krajewski, *Nature* **386**, 156, (1997)
6. A.I. Abramovich, L.I. Koreleva, L.N. Lukina, *Phys. Solid State* **41**, 73, (1999)
7. L.I. Koroleva,Ya.A. Kessler, L.N. Lukina, T.V. Virovets, D.S. Filimonov, *J. Magn. Magn. Mater.* **157**/**158**, 475 (1996).
8. M. Ito, T. Furuta, N. Terada, S. Ebisu, S. Nagata, *Physica B* **407**, 1272, (2012)
9. R.J. Bouchard, P.A. Russo, A. Wold, *Inorg. Chem*. **4**, 685, (1965)
10. A. Kimura, J. Matsuno,J. Okabayashi, A. Fujimori,T. Shishidou,E. Kulatov, T. Kanomata, *Phys. Rev. B* **63**, 224420, (2001)
11. R. Endoh, J. Awaka, S. Nagata, *Phys. Rev. B* **68**, 115106, (2003)
12. Lotgering, F. K.; van Stapele, R. P.; *Solid State Commun*. **1967,** 5,143.
13. Goodenough, J. B.; *J. Phys. Chem. Solids* **1969**, 30, 261.
14. Yamashita, O.; Yamaguchi, Y.; Nakatani, I.; Watanabe, H.; Matsumoto, K.; *J. Phys. Soc. Jpn.* **1979**, 46, 1145.
15. Schöllhorn, R.; *Angew. Chem., Int. Ed. Engl.* **1988**, 27, 1392.
16. Kimura, A.; Matsuno, J.; Okabayashi, J.; Fujimori, A.; Shishidou, T.; Kulatov, E.; Kanomata, T.; *J. Electron Spectrosc. Relat. Phenom.,* **2001**, 114–116, 789.
17. Kamihara, A.; Matoba, M.; Kyomen, T.; Itoh, M.; *Solid State Commun*. **2004**, 132, 247.
18. Bodenez, V.; Dupont, L.; Laffont, L.; Armstrong, A. R.; Shaju, K. M.; Bruce, P. G.; Tarascon, J.-M.; *J. Mater. Chem.,* **2007**, 17, 3238.
19. Matsumoto, N.; Hagino, T.; Taniguchi, K.; Chikazawa, S.; Nagata, S.; *Physica B* **2000**, 284-288, 1978.
20. Okada, H.; Koyama, K.; Watanabe, K.; *J. Alloys Cmpd*., **2005**, 403, 34.
21. Imanishi, N.; Inoue, K.; Takeda, Y.; Yamamoto, O.; *Journal of Power Sources,* **1993**, 43-44, 619.
22. Sinha, S.; Murphy, D. W.; *Solid State Ionics* **1986**, 20, 81.
23. Bodenez, V.; Dupont, L.; Morcrette, M.; Surcin, C.; Murphy, D. W.; Tarascon, J.-M.; *Chem. Mater.* **2006,** 18, 4278.
24. Schöllhorn, R.; Payer, A.; *Anqew. Chern. Int. Ed. Engl*. **1985**, 24, 67.
25. James, A. C. W. P.; Ellis, B.; Goodenough, J. B.; *Solid State Ionics* **1988**, 27, 45.
26. Koyama, T.; Sugita, H.; Wada, S.; Miyatani, K.; Tanaka, T.; Ishikawa, M.; *Physica B*, **2000**, 284-288, 1513.
27. Kariya, F.; Ebisu, S.; Nagata, S.; *J. Solid State Chem*, **2009**, 182, 608.
28. Gabay, M.; Toulouse, G.; *Phys. Rev. Lett*., **1981**, 47, 201.
29. de Almeida, J. R. L.; Thouless, D.J.; *J. Phys. A*, **1978**, 11, 953.